

a

Captions to color illustrations

Figure 1.3.4. Mixing of two immiscible polymers. The image-processed Fourier filtered transmission electron micrograph shows poly(butadiene) (black and light blue) domains in a poly(styrene) matrix (light grey). The black domains correspond to the domains not connected to the boundary. The volume fraction of poly(butadiene) is 0.312 and the average cluster size is $4.8 \mu\text{m}$. (Reproduced with permission from Sax (1985).)

Figure 1.3.5. Mixing below the mixing transition in a mixing layer, visualization by laser induced fluorescence [the term 'mixing transition' refers to the onset of small scale three-dimensional motion]. The experimental conditions correspond to a speed ratio $U_2/U_1 = 0.45$, and a Reynolds number based on the local thickness of 1,750. A fluorescent dye is pre-mixed with the low speed free stream. Laser induced fluorescence allows the measurement of the local dye concentration, (a) single vortex, (b) pairing vortices. (Reproduced with permission from Koochesfahani and Dimotakis (1986).)

Figure 7.3.10. Manifolds corresponding to various values of μ , (a) $\mu = 0.3$, and (b) $\mu = 0.5$. (c) Magnified view of the stable and unstable manifolds of two period-1 points for $\mu = 0.5$ (see 7.3.10(a)). The unstable manifolds of the central point are shown in red, the stable manifold in yellow, the unstable manifolds of the outer point are shown in green, the stable manifold in light blue. The figure shows the results for 15 iterations. More iterations would make the picture hard to visualize; the number of points in the manifolds of the central point is 4,000, the number of points in the manifolds of the outer point is 2,000. (d) Magnified view of the manifolds near the transition to global chaos (the figure corresponds to $\mu = 0.38$). Note that the manifolds of the central and outer points intersect slightly. Compare with Figure 7.3.2. (Reproduced with permission from Khakhar, Rising, and Ottino (1987).)

Figure 7.4.4. Comparison of Poincaré sections and experiments ($\theta_{\text{out}} = 360^\circ$): (a) Poincaré section corresponding to 8 initial conditions and 1,000 iterations; the symmetry of the problem produces a total of 16,000 points. (b) Experiments corresponding to the stretching of a blob initially located in the neighborhood of the period-1 hyperbolic point for 15 periods.

Figure 7.4.5. Similar comparison to that of Figure 7.4.4 except that $\theta_{\text{out}} = 180^\circ$: (a) Poincaré section; colored points reveal that the initial conditions 'do not mix' even for a large number of periods, e.g., see magenta points; (b) corresponding experimental result for 10 periods (blob initially located in the neighborhood of the period-1 hyperbolic point), in this case, the blob does not invade the entire chaotic region.

Figure 7.4.6. Comparison of two Poincaré sections identical in all respects, except that the angular displacement θ_{out} of the outer cylinder in case (a) is 165° whereas in case (b) it is 166° . The value of θ_{in} is such that $\Omega_{\text{in}}/\Omega_{\text{out}} = -2$. The initial placement of colored points is the same in both cases.

Figure 7.4.7. (a) Location of periodic points, and (b) corresponding Poincaré section ($\theta_{\text{out}} = 180^\circ$). The crosses represent hyperbolic points, the circles elliptic points. The period of the point is indicated by the color; green = 1, red = 2, blue = 3, orange = 4, yellow = 5, ... White results due to 'superposition' of nearby points of different order.

Color illustrations

b

Figure 7.4.10. Poincaré sections corresponding to the angular histories of Figure 7.4.9: (a) square ($\theta_{\text{out}} = 180^\circ$), (b) \sin^2 , (c) sawtooth, and (d) $|\sin|$. The initial placement of colored points is the same in all cases. Note that whereas the large scale features are remarkably similar the distribution of colors reveals some local differences.

Figure 7.4.11. Stretching map corresponding to square history and 10 periods. The figures were constructed by placing two vectors per pixel and averaging over 10^2 initial orientations. In (a) $\theta_{\text{out}} = 180^\circ$ and the white regions correspond to stretching of greater than 50; in (b) $\theta_{\text{out}} = 360^\circ$ and the cut-off value is 5,000. Figure (a) should be compared with 7.4.8 and 7.4.5, (b) with 7.4.4(a,b).

Figure 7.5.7. An experiment similar to that of Figure 7.5.5 showing an island at the point of bifurcation ($T = 48.2$ s, displacement 970 cm, $Re = 1.2$, $Sr = 0.08$). This structure is characteristic of a golden mean rotation speed.

Figure 7.5.8. Partial structure of periodic points corresponding to the system of Figure 7.5.2(d), A = hyperbolic period-1; B = elliptic period-2; C = hyperbolic period-2; D = elliptic period-4; and E represents a hole of period-1. Note that the circles represent elliptic points and the squares hyperbolic points. The full white lines connect two elliptic points to a central hyperbolic point; all three points move as a unit. The broken lines connect two period-2 hyperbolic points to a period-1 hyperbolic point; the two period-2 hyperbolic points were born from the period-1 hyperbolic point. The two period-2 hyperbolic points interchange their positions after one period.

Figure 7.5.9. Illustration of reversibility in regular and chaotic regions. The mixing protocol corresponds to Equation (7.5.1a,b) with a period of 30 s. (a) is the initial condition at which the vertical line is placed in the chaotic region, while the oblique line is placed in the regular region. (b) shows the lines after two periods. Note that the stretching and bending of the line placed in the regular region is very small, and that the line is merely translated. On the other hand, the line placed in the chaotic regions suffers significant stretching. (c) shows the state of the system after being reversed for two periods. Clearly, the line in the regular region managed to return to its initial location successfully, however, the line in the chaotic region loses its identity due to the magnification of errors in the experimental set-up.

c

Color illustrations

Fig. 1.3.4

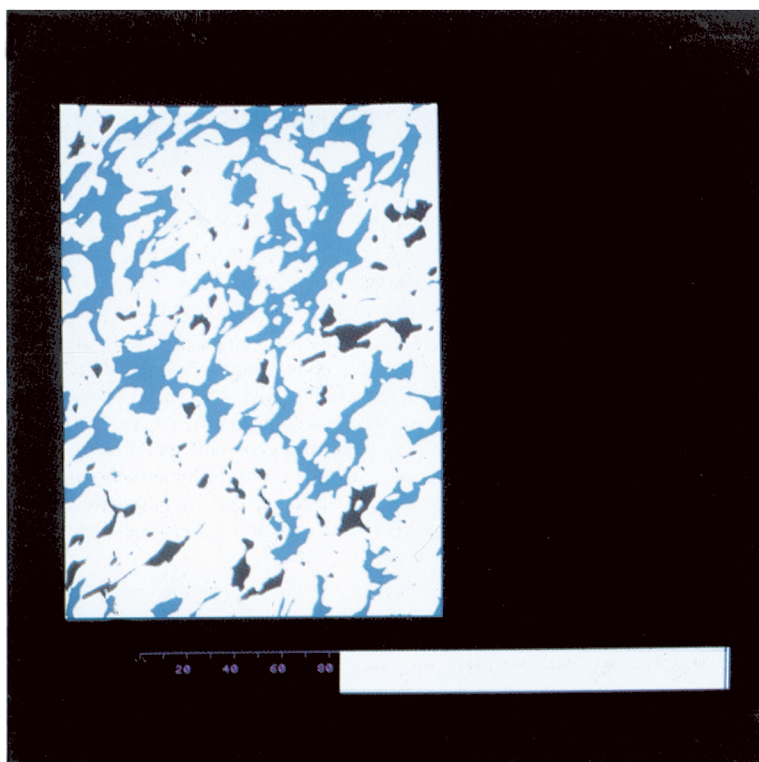


Fig. 1.3.5

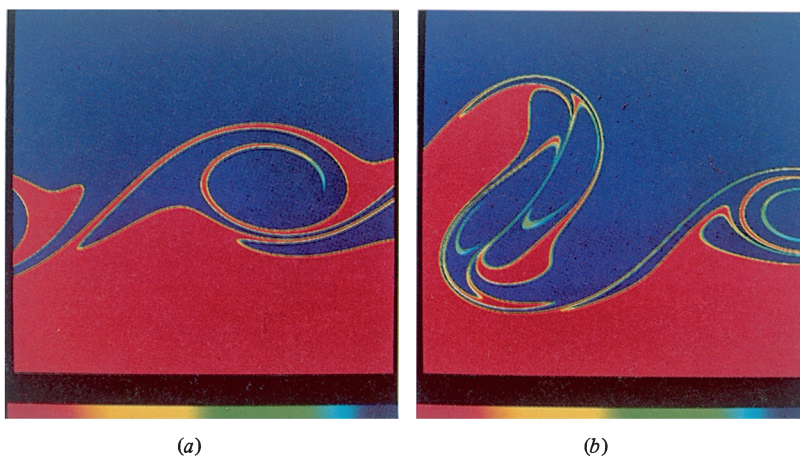
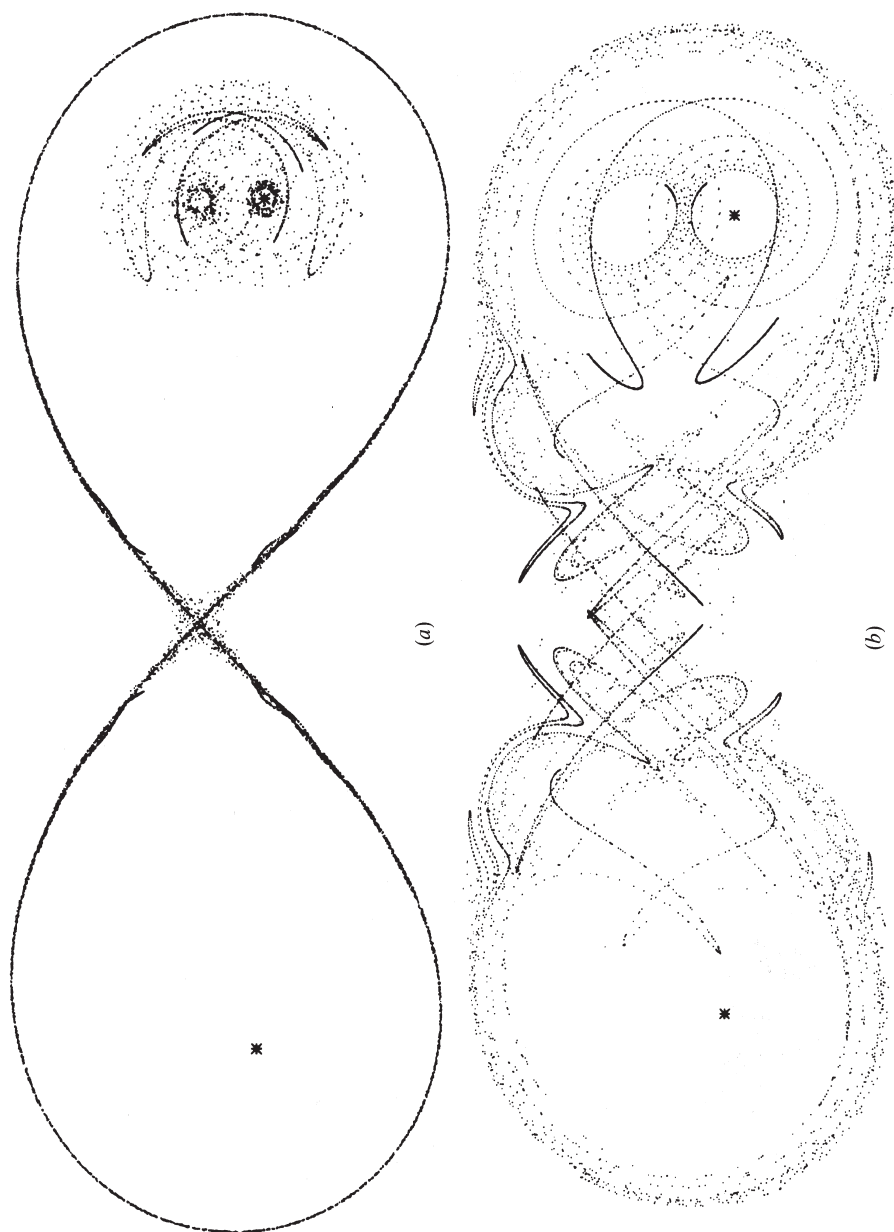
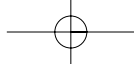


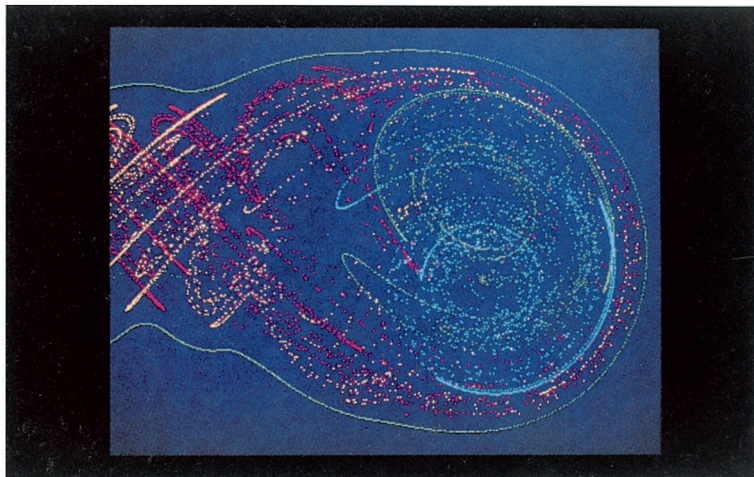
Fig. 7.3.10



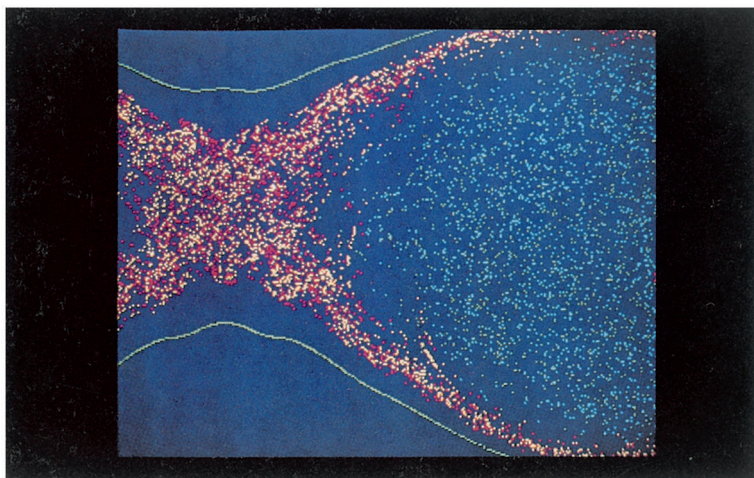


e

Color illustrations



(c)

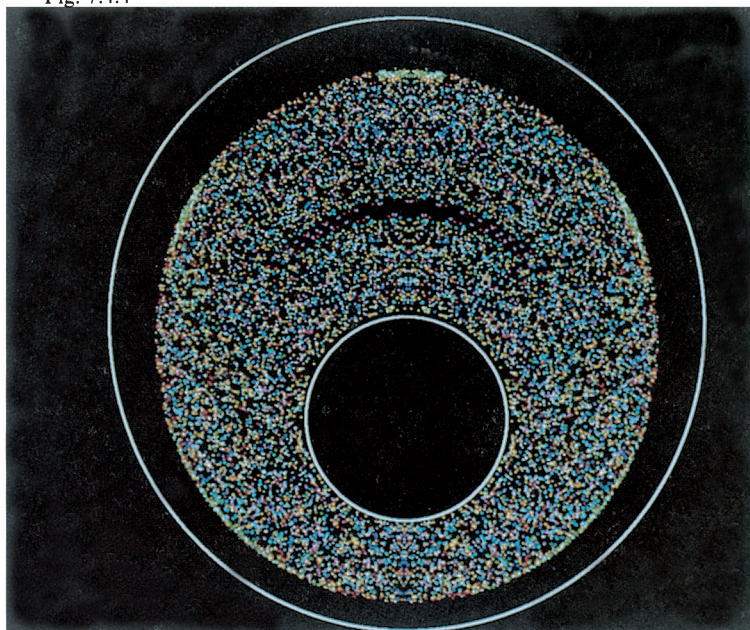


(d)

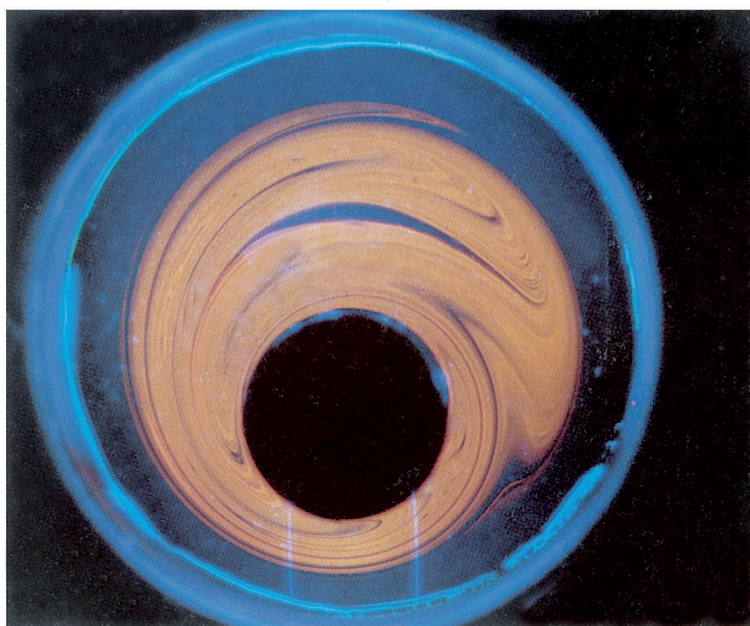
Color illustrations

f

Fig. 7.4.4



(a)

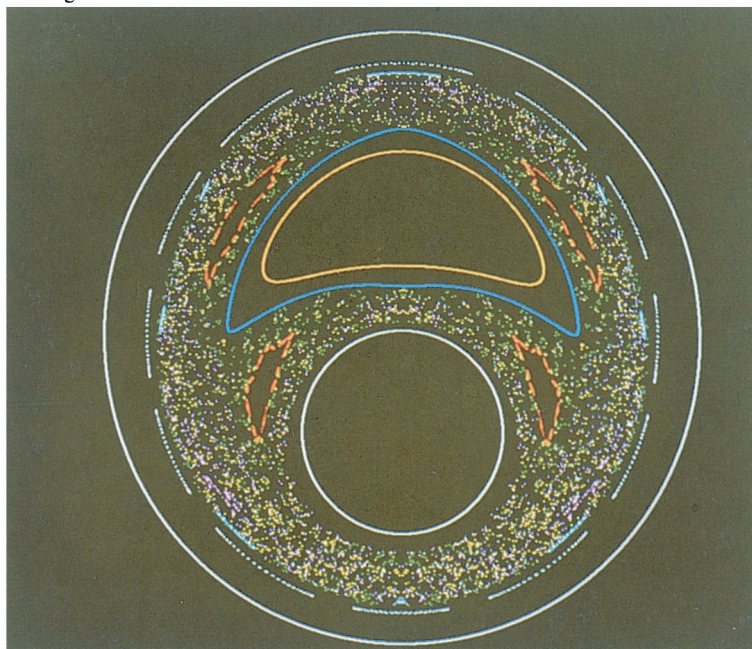


(b)

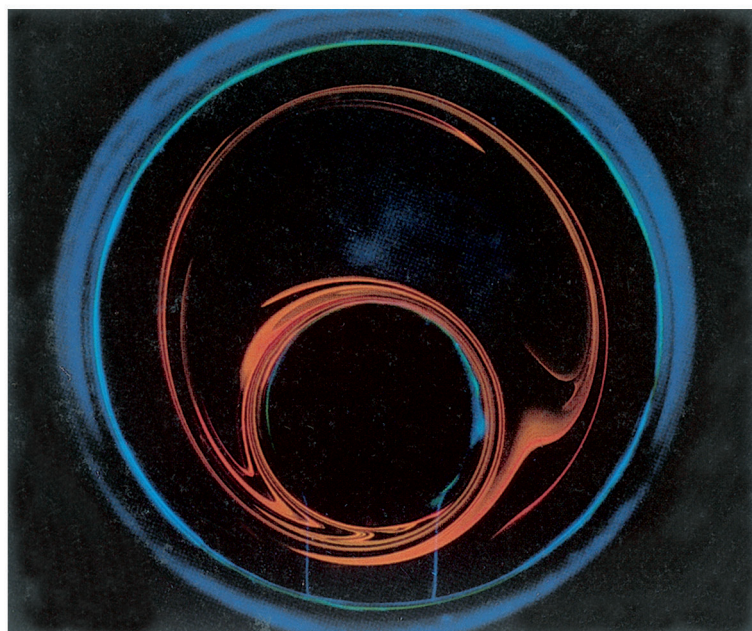
g

Color illustrations

Fig. 7.4.5

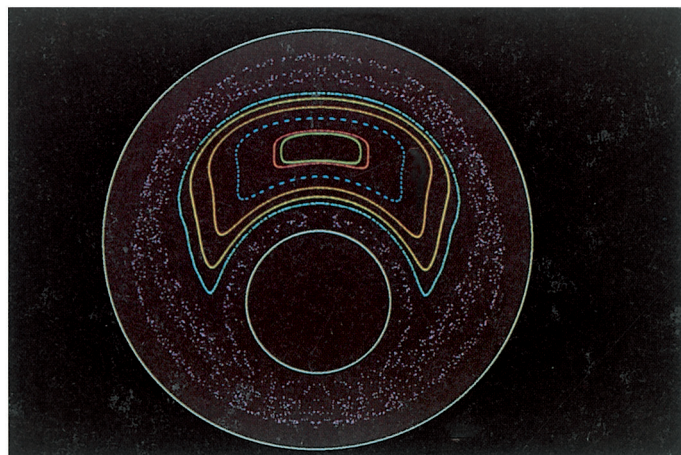


(a)

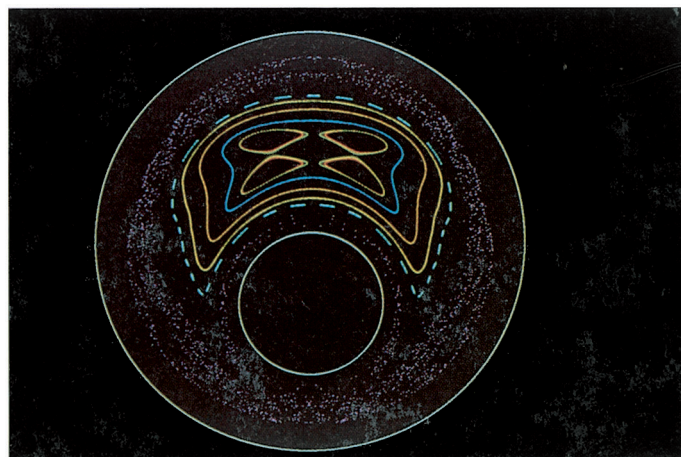


(b)

Fig. 7.4.6



(a)

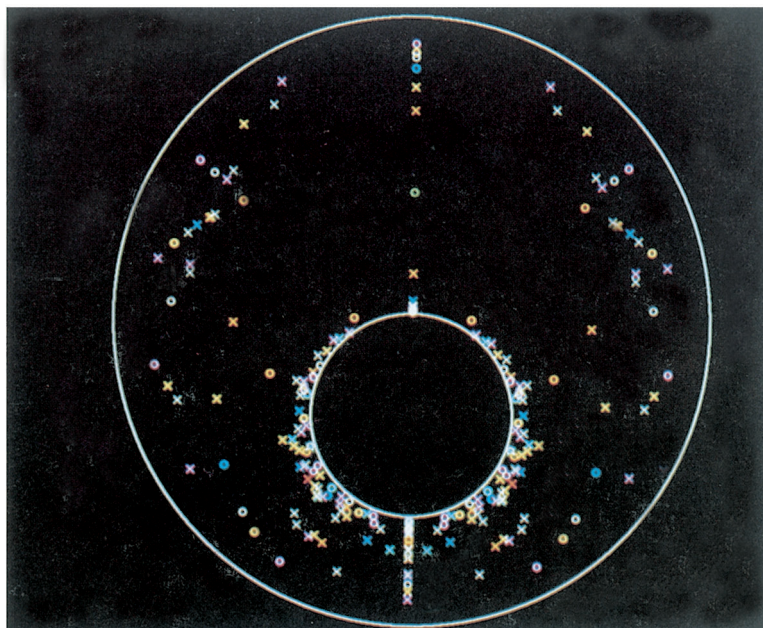


(b)

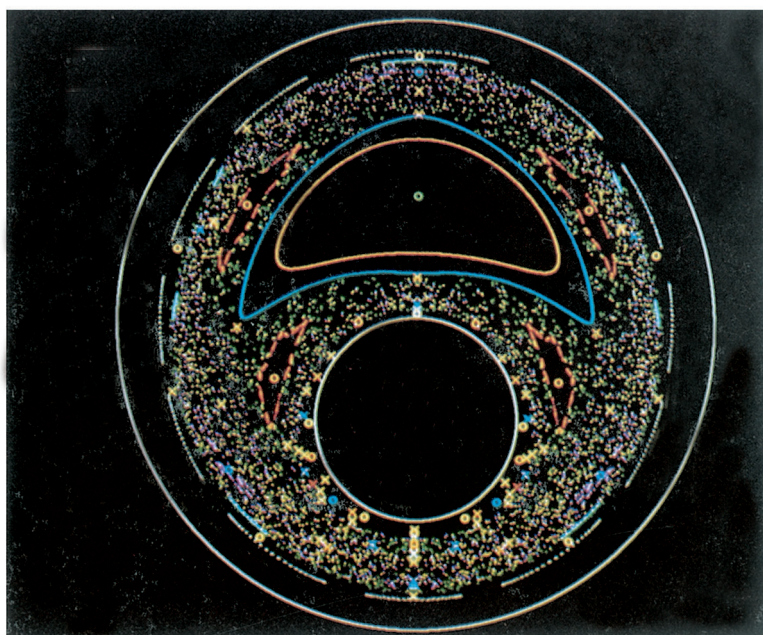
i

Color illustrations

Fig. 7.4.7

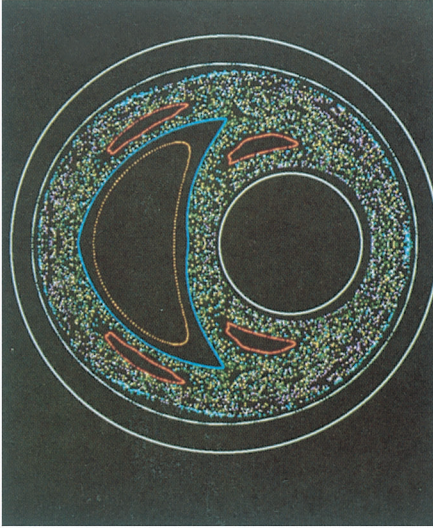


(a)

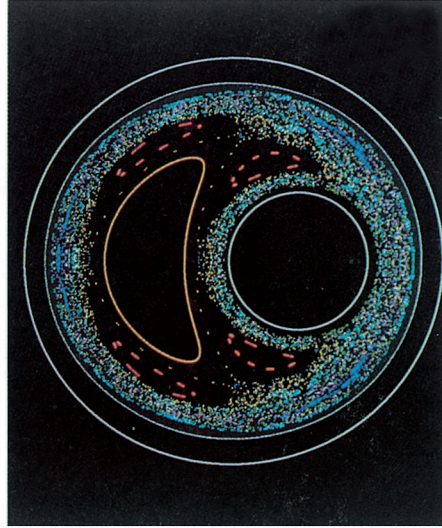


(b)

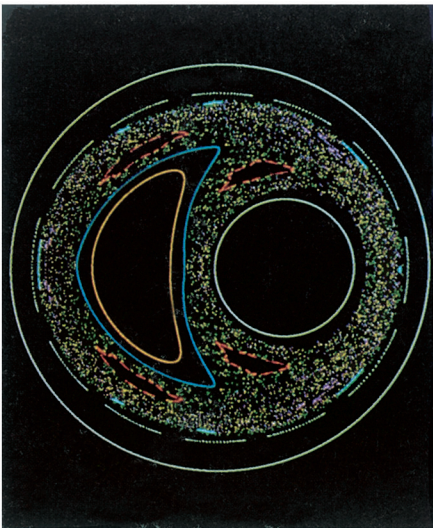
Fig. 7.4.10



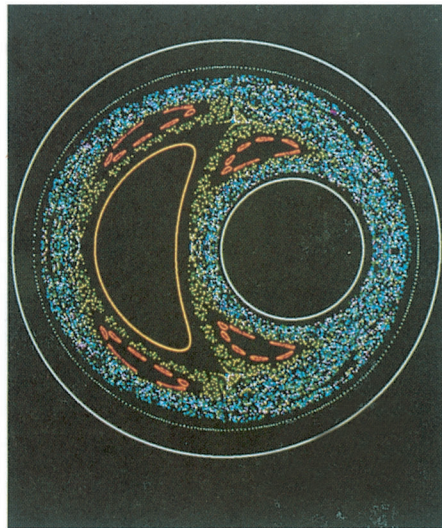
(a)



(b)



(c)

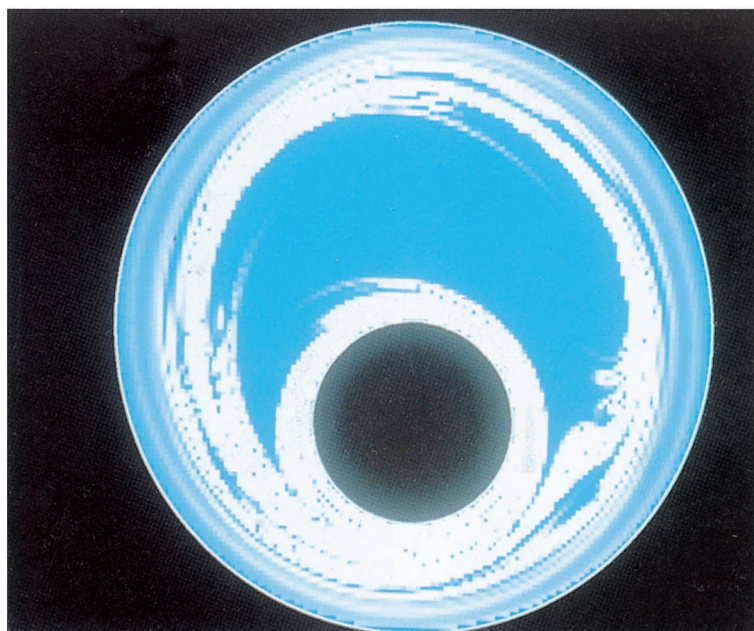


(d)

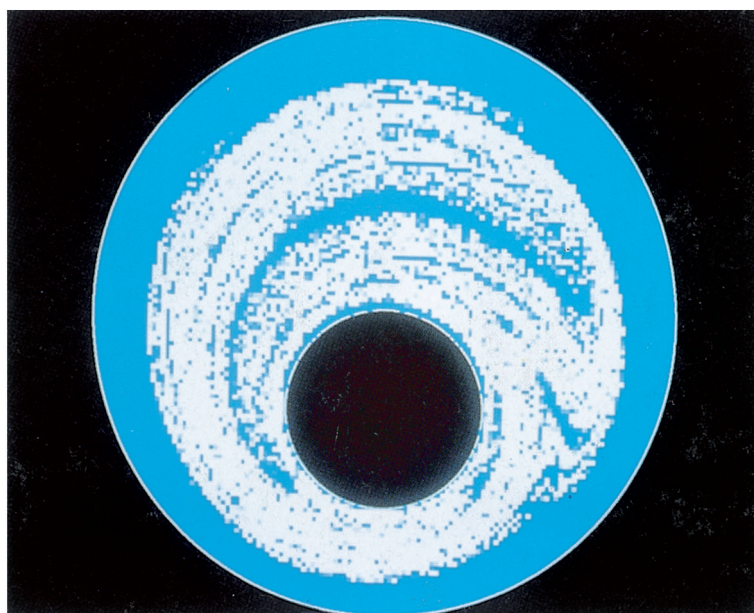
k

Color illustrations

Fig. 7.4.11



(a)

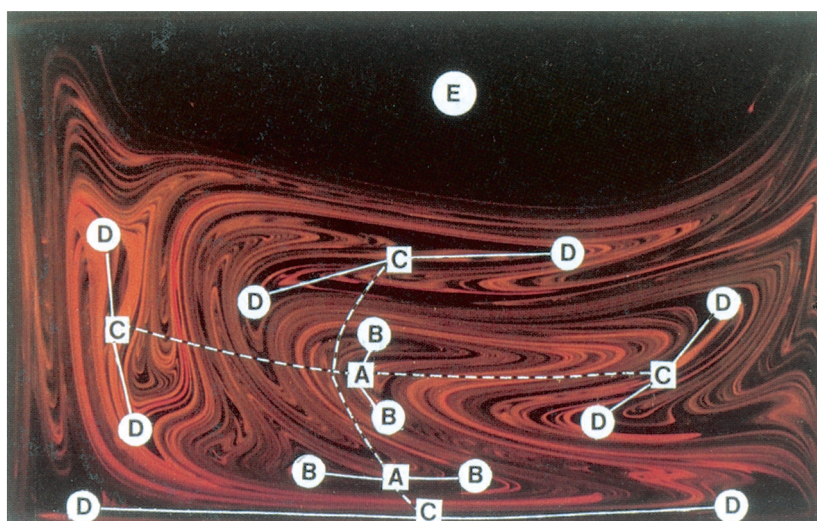


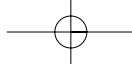
(b)

Fig. 7.5.7



Fig. 7.5.8





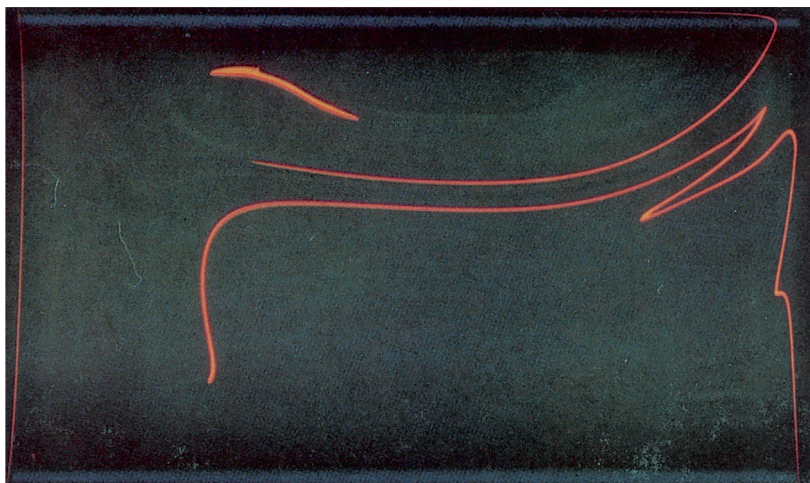
m

Fig. 7.5.9

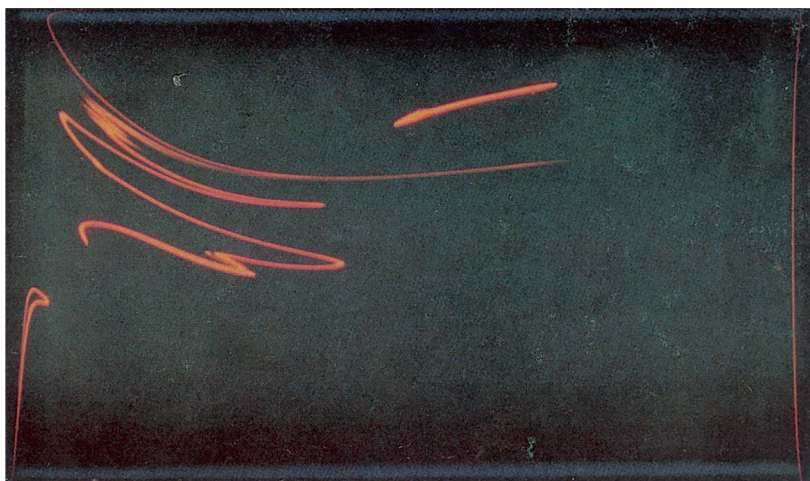
Color illustrations



(a)



(b)



(c)

